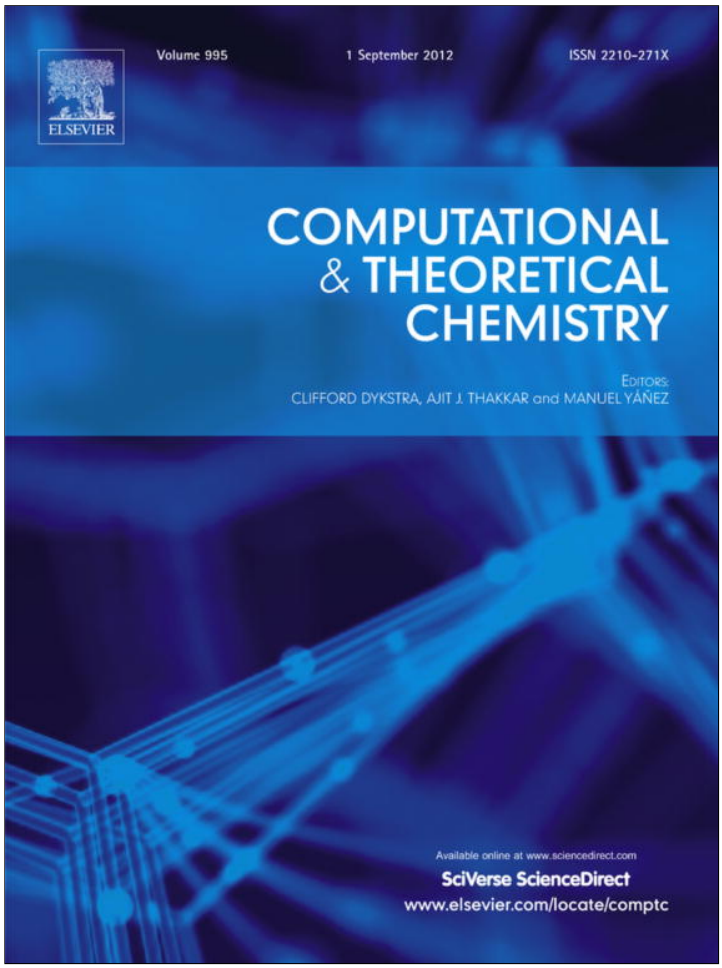

Computational and Theoretical Chemistry 995 (2012) 66–74

Contents lists available at SciVerse ScienceDirect

Computational and Theoretical Chemistry

journal homepage: www.elsevier.com/locate/comptc

Vibrations of polythiophenes

Sergiu C. Pop, Titus A. Beu *

Faculty of Physics, University "Babeş-Bolyai", 400084 Cluj-Napoca, Romania

ARTICLE INFO

Article history:
Received 27 March 2012
Received in revised form 26 June 2012
Accepted 27 June 2012
Available online 5 July 2012

Keywords:
Polythiophenes
IR and Raman spectra
DFT

ABSTRACT

Structural and vibrational properties of thiophene oligomers up to the dodecamer have been investigated by first principles calculations. The main goal is to provide more detailed interpretations of the infrared and Raman spectra, extending the insights to odd-sized polythiophenes, which have not been treated so far. The calculated electronic, geometric, and vibrational features show better consistency and agreement with experimental data than previously published theoretical results.

1. Introduction

The very special characteristics of π-conjugated polymers make them suitable for optical and electronic applications, such as Organic Light-Emitting Diodes (OLEDs) [1–3], field effect transistors (FET) [4], and photovoltaic devices [5,6], motivating the efforts for deeper insight into their fundamental physical and chemical properties [7].

Polythiophenes can be seen as prototypes of organic π-conjugated polymers and their study has gained considerable momentum due to their semiconducting [8] and non-linear optical properties [9]. In particular, hexathiophene was used to fabricate thin film transistors with promising performances for large area electronic circuits.

In order to optimize the growth process and morphology, as well as the optical and electronic properties of thin films based on thiophene oligomers, a comprehensive study of the physical and chemical properties of the polymers is required. A central role is played by the vibrational properties, which, being most sensitive to conformational changes induced, for example, by doping, may provide important structural information susceptible to be useful in developing new applications.

The intramolecular vibrations of the three smallest even-sized polythiophene oligomers have been studied in detail by Zerbetto et al. [10] by combining Inelastic Neutron Scattering (INS), infrared (IR) and Raman experiments, and calculations. Through refinement of ab initio force fields at Hartree Fock level, the three types of vibrational spectra of each oligomer have been fairly well reproduced. The fitting procedure implied iteration over: (1) calculation of vibrational frequencies and assignment on the basis of the experimental IR and Raman activity; (2) fitting of the INS profile; (3) calculation of IR and Raman spectra with the new normal modes and the ab initio derivatives of the dipole moment and the polarizability. This preliminary work relied on the accurate assignment of the vibrational features of the dimer and tetramer and on the transferability of the model to higher oligomers. In a more recent paper, Degli Esposti et al. [11] present highly resolved experimental IR and Raman spectra of α-T6 (alpha hexathiophene) single crystal and their calculations using a scaled ab initio force field at Hartree Fock level. Insight into the molecular phonons is gained, including vibrations which are silent in optical spectroscopies.

In the present paper we present detailed calculations of structural and vibrational properties of polythiophenes up to the dodecamer based on higher level first principles methods than the ones employed previously in similar studies and extend the investigations from the hitherto considered even-sized to odd-sized oligomers. One of the aims has been to discriminate size and symmetry-specific trends in the electronic structure and IR and Raman spectra of the studied polythiophenes.

The article is structured as follows: Section 2 gives an outline of the Density Functional Theory (DFT) methodology used, including the rationale for choosing the exchange–correlation functional and the basis set; Section 3 presents the optimized molecular structures and the vibrational analysis, with detailed comparisons with experimental and theoretical IR and Raman spectra from the literature; in Section 4 the main conclusions of this work are presented.

2. Theoretical methodology

As already mentioned, the present study focuses on the accurate first principles calculation of the equilibrium structures, normal modes, and vibrational spectra of the 12 smallest polythiophene oligomers.

* Corresponding author. Tel.: +40 752 441 608.
E-mail address: titus.beu@phys.ubbcluj.ro (T.A. Beu).

2210-271X/$ - see front matter © 2012 Elsevier B.V. All rights reserved.
http://dx.doi.org/10.1016/j.comptc.2012.06.031

Whereas previous similar work concerned only even-sized molecules [10], we have considered equally the odd-sized ones.

All implied DFT calculations, both structural and vibrational, have been carried out using the GAUSSIAN 03 package [12]. An initial preparatory phase consisted in the systematic assessment of various combinations of exchange–correlation functionals and basis sets with a view to optimally reproduce experimental structural and vibrational features. Specifically, we have employed the popular B3LYP exchange–correlation functional [13] and for comparison the PBE gradient-corrected correlation functionals of Perdew et al. [14]. In terms of basis sets, we have used the all-electron polarized basis set 6-31G(d) and, as less expensive variant, the effective core potential basis-set CEP-31G(d). For all considered oligomers, the 6-31G(d) basis set requires significantly more computational resources, but provides considerably more accurate vibrational spectra. The papers we relate our results to have reported without exception data obtained at Hartree–Fock level, using either the 3-21G(d) or 6-31G(d) basis sets [11,15].

Even though we considered basis sets which are generally considered suitable for the present type of molecules, we encountered convergence difficulties for the larger oligomers, fact which was already mentioned in the literature [10].

Since the typical experiments deal with molecular crystals, bonded by van der Waals forces, the measured vibrational spectra include at low frequencies features due to the corresponding lattice phonons. Our calculations, however, are carried out for isolated species and, thus, account only for the IR and Raman-active vibrations.

3. Results and discussion

3.1. Geometries

With a view to analyze consistently and with manageable computational effort also larger oligomers than the hexamer, we have initially carried out calculations using the CEP-31G(d) basis set, taking advantage of the reduced computational costs involved by modeling the core electrons with an effective potential. However, already the optimized bond lengths turned out to be affected by errors as compared to those obtained with the 6-31G(d) basis set and, moreover, showed a level-out tendency, not differentiating between the in-ring C—C bonds. Given the already appreciable geometrical inaccuracies, the vibrational spectra departed even more from the superior 6-31G(d) results. Consequently, we performed all structure and spectroscopy calculations reported here using the 6-31G(d) basis set.

Among the technical aspects which define our work in comparison to other publications, we mention the consistent application of symmetry constraints and the critical assessment of the performance of different exchange–correlation functionals. Specifically, imposing symmetry conservation, namely C_{2h} for even-size oligomers and C_{2v} for the odd-size ones, lead to improved convergence and increased computational efficiency. On the other hand, the B3LYP and PBE exchange–correlation functionals turn out to favor a cancelation of errors, though in different spectral regions (as will be discussed below), in such a way that there is no need of scaling the vibrational frequencies to match them with published experimental data.

Concerned with the degree to which different exchange–correlation functionals prove appropriate for the particular case of polythiophenes, we performed comparative calculations with the B3LYP and PBE functionals. The optimized geometrical structure, the atom numbering, as well as the HOMO and LUMO orbitals, have been depicted in Fig. 1 for the pentamer (as prototype of odd-size oligomer) and in Fig. 2 for the hexamer (as prototype of even-size oligomer). In geometrical terms, as seen from. Table 1, where the relative deviations of several bond lengths of hexathiophene from experimental values [10] are listed, there emerged a slightly better ability (typically amounting to 0.01 Å) of the B3LYP functional to reproduce the inter-cycle C—C bond [16,17]

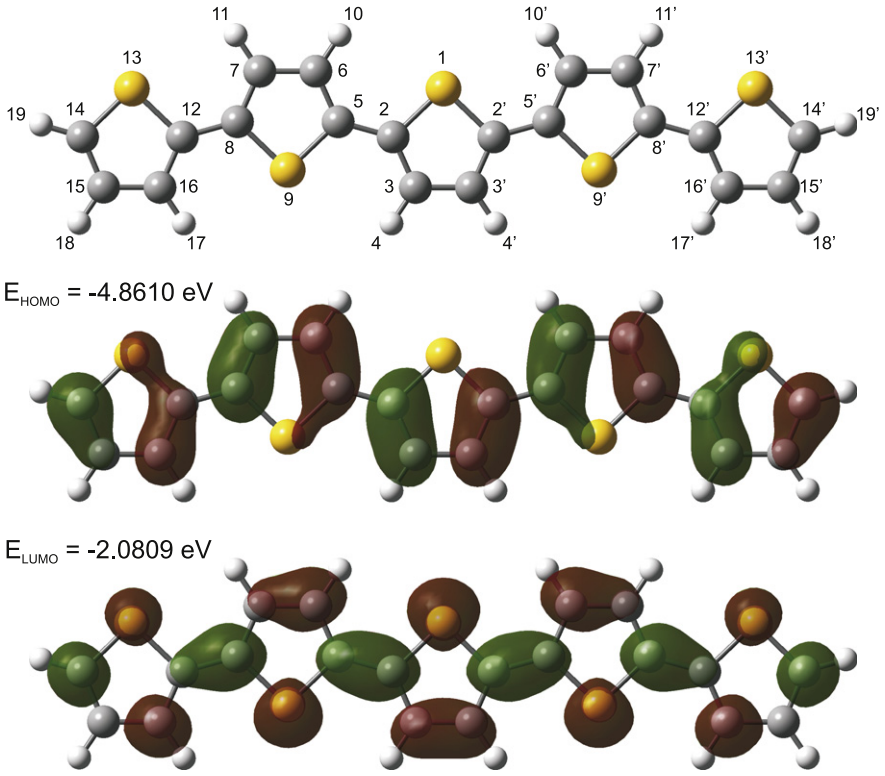

Fig. 1. Numbering scheme and HOMO–LUMO orbitals for pentathiophene obtained with the PBE functional.

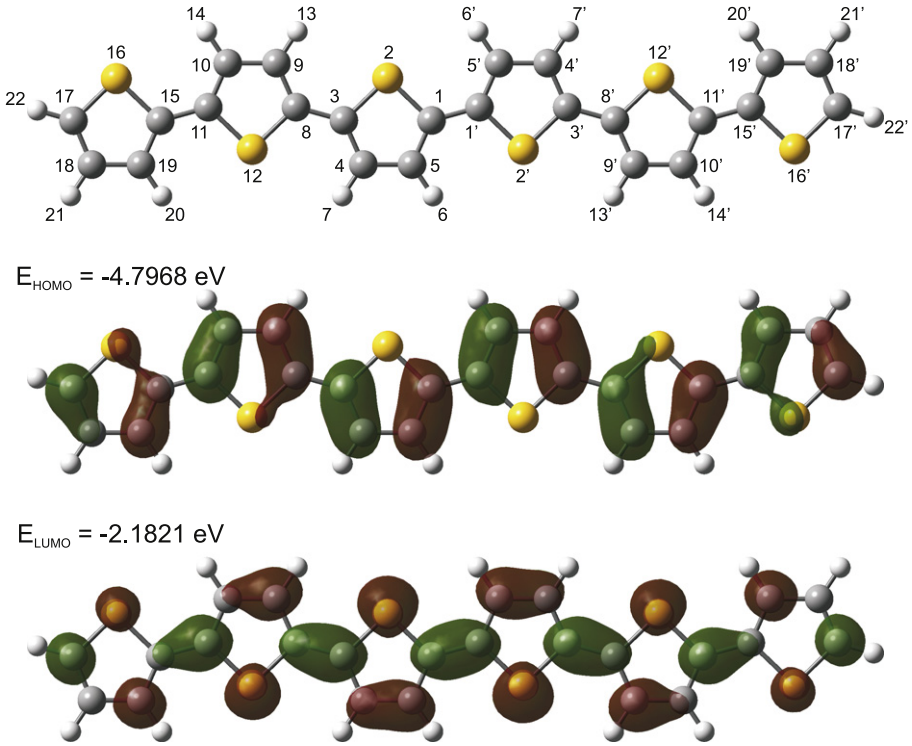

Fig. 2. Numbering scheme and HOMO–LUMO orbitals for hexathiophene obtained with the PBE functional.

Table 1
Representative in and inter-cycle C—C and C—S bond lengths of hexathiophene resulted from experiments [10] and calculated with the B3LYP and PBE exchange–correlation functionals.

	Exp. (Ref. [10]) Å	B3LYP error (%)	PBEPBE error (%)
C1C1′	1.445(9)	−0.4	−0.6
C3C8	1.45(1)−1.46(1)	−1.0	−1.2
C11C15	1.45(1)	−0.40	−0.6
C1S2	1.730(7)−1.731(7)	1.6	1.8
S2C3	1.733(8)−1.739(8)	1.3	1.4
C11S12	1.729(7)−1.733(7)	1.5	1.7
C8S12	1.733(7)−1.742(8)	1.2	1.4
C15S16	1.719(8)−1.726(8)	2.0	2.2
C17S16	1.704(9)−1.711(9)	1.6	1.6
C1C5	1.37(1)−1.38(1)	0.5	1.4
C3C4	1.36(1)	1.5	2.4
C8C9	1.36(1)	1.5	2.4
C10C11	1.38(1)	−0.1	0.8
C15C19	1.38(1)−1.40(1)	−0.8	0.1
C17C18	1.31(1)−1.32(1)	3.9	4.7
C4C5	1.40(1)−1.41(1)	0.6	0.4
C9C10	1.40(1)	0.9	0.8
C18C19	1.41(1)−1.42(1)	0.5	0.5

and C—S bonds [18]. On the other hand, the PBE-based calculations provided closer agreement with the experiments for the in-ring double C=C bonds and the bonds in between, particularly for the ones opposed to the sulphur atoms S2, S12, and S16 (ex. C4C5, C9C10, and C18C19). Overall, the experimental bond lengths are fairly reproduced by both functionals, with the largest deviations amounting to about 2% and occurring for bonds involving sulphur atoms. Previous calculations on pure polythiophenes [10] have been performed at the Hartree Fock level with two different basis sets, 3-21G(d) and the 6-31G(d) (depending on the length of the molecular chain), and agree less with the experimental geometrical features.

As for the HOMO and LUMO orbitals, Figs. 1 and 2 show them to be always oriented transversely and, respectively, longitudinally to the main chain axis, both for even and odd-size oligomers alike. Moreover, we found that similar vibrational modes (discussed in more detail in the next section) develop with increasing size not only, separately, for even or odd-size polythiophenes, but also for the consecutive ones.

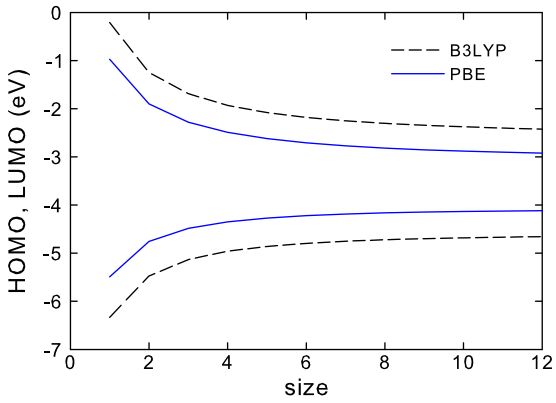

Fig. 3. HOMO and LUMO energies for the thiophene oligomers up to the dodecamer.

As can be seen in Fig. 3, the bandgap calculated with the B3LYP functional is in asymptotic agreement with data published by other authors [18–20] and agrees fairly with the experimental bandgap of 2.21 eV reported for hexathiophene by Chung et al. [21].

3.2. IR and Raman spectra

The straightforward way of understanding the vibrational fingerprints of oligothiophene chains is to compare the experimental data with the results of ab initio calculations. A significant aspect of the present calculations is that they assume molecular systems

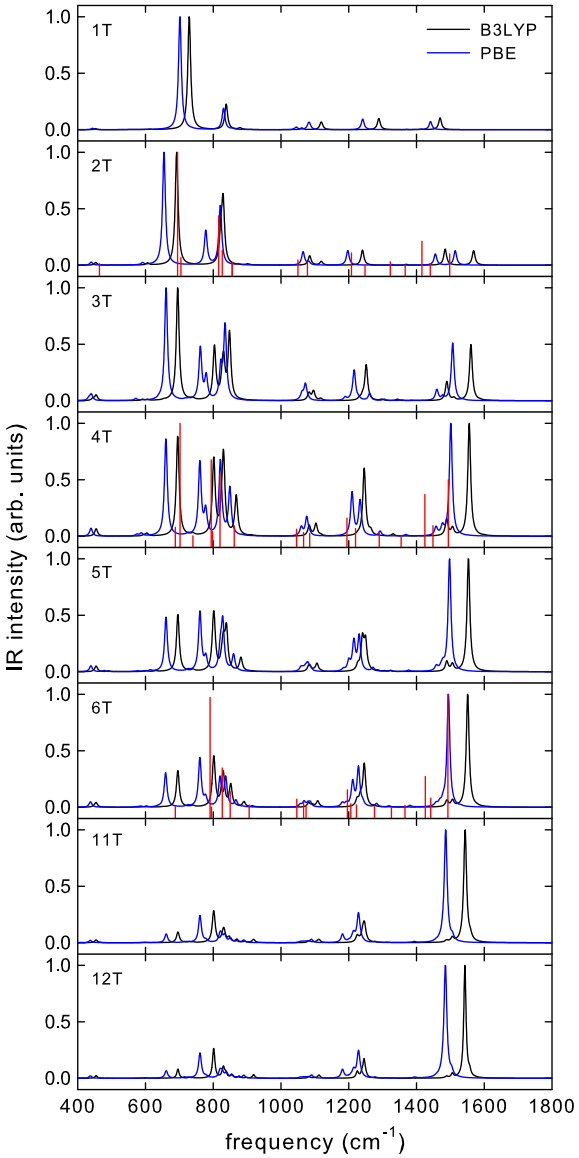

Fig. 4. IR spectra for the oligotiophenes obtained with the basis set 6-31G(d) imposing symmetry conservation and experimental peaks with drop lines [10].

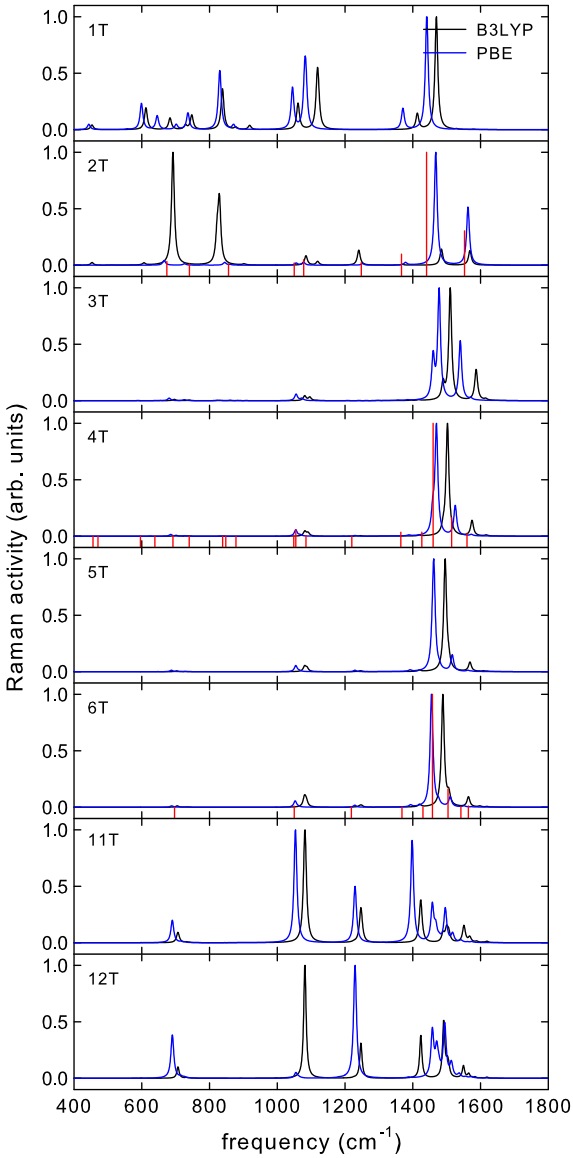

Fig. 5. Raman spectra for the oligotiophenes obtained with the basis set 6-31G(d) imposing symmetry conservation and experimental peaks with drop lines [10].

in gas phase, while the experiments are typically performed in condensed phase. As mentioned before, our calculations are able to reproduce the experimental vibrational modes and give better results in cases where the natural symmetry of the considered compounds (C_{2h} and C_{2v}) is imposed and conserved.

We present comparatively in Figs. 4 and 5 our calculated IR and Raman spectra for the oligothiophenes up to the hexamer, as well as for the 11-mer and 12-mer. Larger oligomers present obviously more crowded spectra. As in the case of the geometry optimization, the results obtained with the 6-31G(d) basis set provide the closest agreement with the experiment, and are exclusively referred to in the following.

In order to simplify the subsequent discussion and to establish links with certain categories of vibrational modes, we divide conventionally the whole IR and Raman spectral range for the considered polythiophenes into three distinct regions. The first region extends up to 1000 cm^{-1}, is characterized mainly by out-of-plane vibrations, but also by in-plane modes at the blue[1] end, is quite crowded in terms of IR-active vibrations, but only moderately populated with Raman features. The second region ranges between 1000 cm^{-1} and 1400 cm^{-1} and is moderately occupied by IR

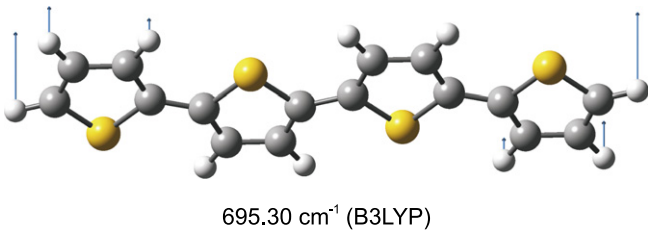

Fig. 6. Out-of-plane IR modes of the tetramer corresponding to the experimental peak located at 702 cm^{-1} [10], calculated with the B3LYP functional.

spectroscopic features, while Raman modes are better represented, especially for the monomer and the large oligomers. The third region spreads up to 1600 cm^{-1}, is well populated both with IR and Raman-active modes, which correspond mostly to in-plane motions.

As a preliminary general remark emerging from Figs. 4 and 5 is the fair agreement of our calculations for the three smallest even-size

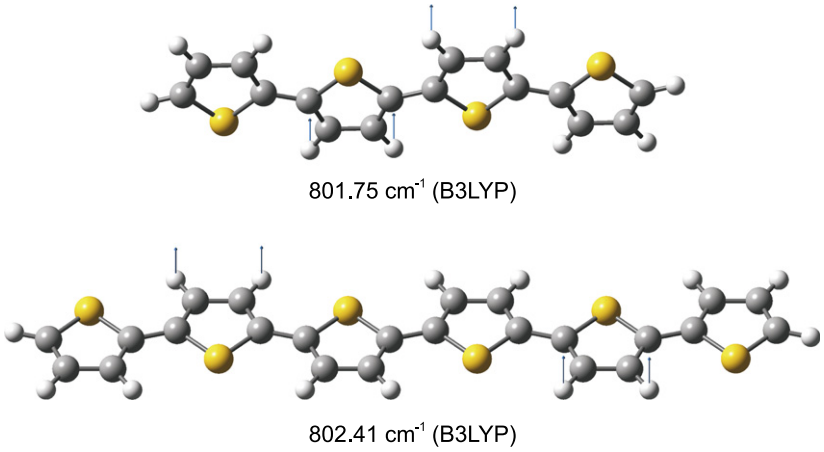

Fig. 7. Out-of-plane IR modes of the teramer and hexamer corresponding to the experimental peaks located at 794 and 791 cm^{-1} [10], obtained with the B3LYP functional.

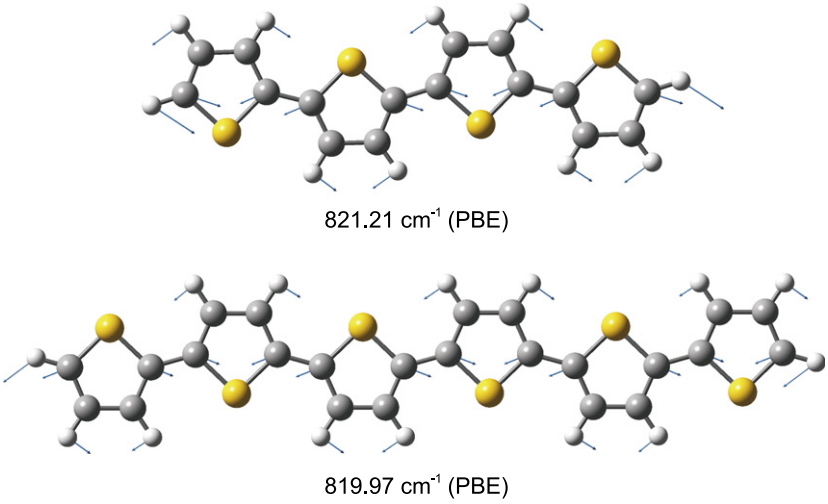

Fig. 8. In-plane IR modes of the teramer and hexamer corresponding to the experimental peaks located at 818 and 827 cm^{-1} [10], calculated with the PBE functional.

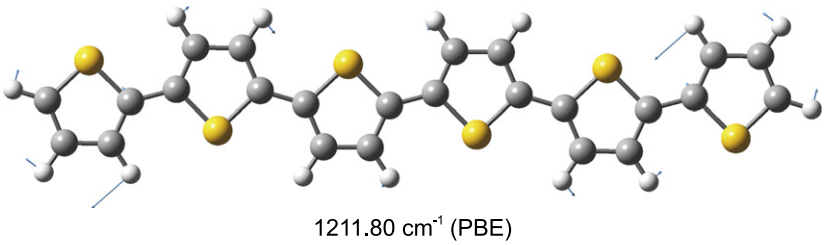

Fig. 9. In-plane IR modes of the hexamer corresponding to the experimental peak located at 1196 cm^{-1} [10], obtained with the PBE functional.

oligomers with the available experimental peaks from the literature (represented with vertical drop lines) [10].

According to the conventional subranges mentioned before, the 600–1000 cm^{-1} region is characterized mainly by out-of-plane ring deformations, bendings involving the C—S bonds, and pyramidalizations [10].

In the 600–700 cm^{-1} subrange a very different response for the first three even oligomers is observed. The dimer, in particular, exhibits in the IR experimental spectrum of Zerbetto et al. [10,23,24] two well-separated features, with the first peak, higher in intensity, situated at 695 cm^{-1} and the second one at 705 cm^{-1}. The peaks are very well reproduced by our B3LYP calculations (Fig. 4) both in terms of position and relative intensity. The out-of-plane vibrational mode corresponding to the more intense peak activates predominantly the H-atoms and conserves the inversion symmetry, with the symmetric H-atoms close to the S-atoms vibrating with the largest amplitudes. The B3LYP frequency for the corresponding trimer mode was found to exactly coincide with the experimental frequency of the dimer.

By increasing the thiophene chain length, the discussed peaks tend to collapse into a unique broad band which implies mainly ring deformations. The calculated IR band of the tetramer peaks approximately at the experimental dimer frequency, while for the hexamer the band is slightly blue shifted, as mentioned by Zerbetto et al. [10]. The normal mode is well reproduced with the B3LYP functional and from Fig. 6 it is seen to be a pure out-of-plane vibration, which involves in-phase, similarly with the dimer, almost exclusively the H-atoms connected to the terminal cy-

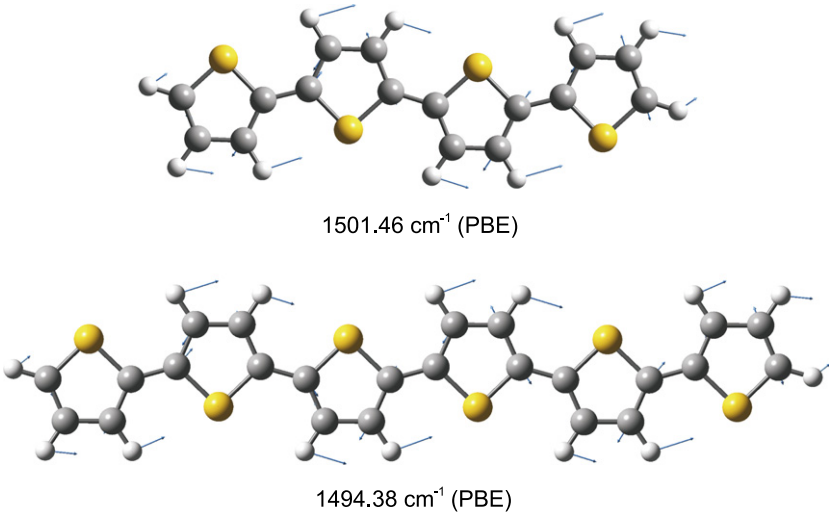

Fig. 10. In-plane IR modes of the teramer and hexamer corresponding to the experimental peaks located at 1494 and 1493 cm^{-1} [10], calculated with the PBE functional.

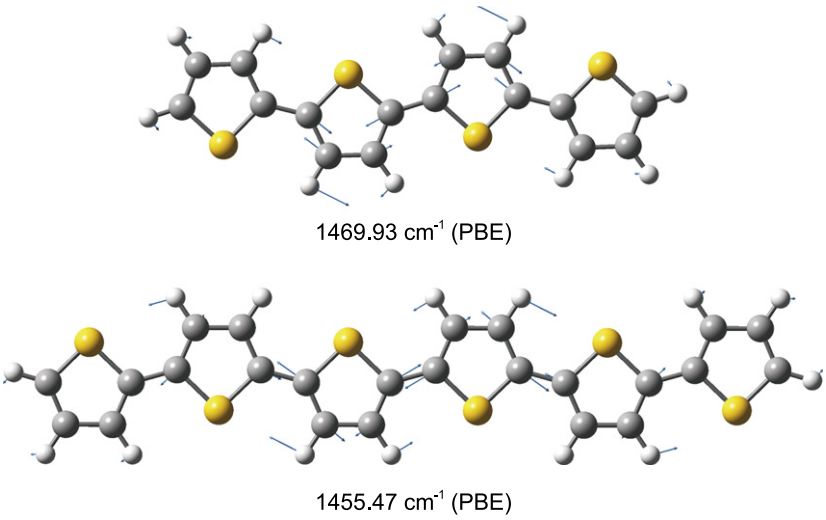

Fig. 11. In-plane Raman modes of the teramer and hexamer corresponding to the experimental peaks located at 1460 and 1458 cm^{-1} [10], obtained with the PBE functional.

cles of the compound, symmetrically to the inversion point. The calculated frequency for the pentamer was found to be exactly the same as for the tetramer.

The out-of-plane IR modes of the tetramer and hexamer corresponding to the experimental vibrations at 794 and 791 cm^{-1} [10] are accurately calculated in our study with the B3LYP functional both in terms of position and decreasing intensities (Fig. 4). As an interesting unifying remark, both in the case of the tetramer and the hexamer, as well as for all higher even oligomers, this IR mode mainly activates translationally in-phase and out-of-plane the H atoms of the symmetrically opposed rings preceding the terminal cycles (Fig. 7).

The experimental IR bands [10,22] situated at 816 cm^{-1} for the dimer, at 818 cm^{-1} for the tetramer and at 827 cm^{-1} for the hexamer arise mainly from staggered in-plane motions of the H atoms and of the C atoms located close to the longitudinal axis of the oligomers. Our calculations turned out to be more precise for this family of normal modes when using the PBE functional (as seen from Fig. 8). This particular frequency was also predicted quite accurately by Palmer [24] (at 824.1 cm^{-1}). The corresponding feature for the pentamer was found in our calculations slightly shifted towards higher frequencies (at 830 cm^{-1}).

There is a technical point worth discussing concerning the Raman-active modes of the dimer below 1000 cm^{-1} (Fig. 5). As measured by Zerbetto et al. [10,23,24] and confirmed experimentally and theoretically by Hermet et al. [25] (using DFT and pseudopotentials), there are, indeed, two, relatively weak peaks grouped around 674 cm^{-1}. Even though we see this double peak both using the B3LYP and PBE functionals, the B3LYP functional overestimates largely its Raman activity, while the PBE functional performs much more realistically, reproducing significantly better both the position and the overall relative activity.

The 1000–1400 cm^{-1} region is characterized mainly by in-plane angle bendings involving the H atoms connected to the terminal cycles. Interestingly, the increase of the chain length (implicitly of the distance between the terminal cycles) appears to reduce the IR intensities, as the coupling between the end cycles diminishes. In this intermediate frequency domain, the experimental IR and Raman features are particularly well reproduced for the even-sized oligomers by the PBE calculations (Figs. 4 and 5). As for the trimer and pentamer, for which there is no experimental evidence, the calculated frequencies lie close to those of the dimer and tetramer, respectively.

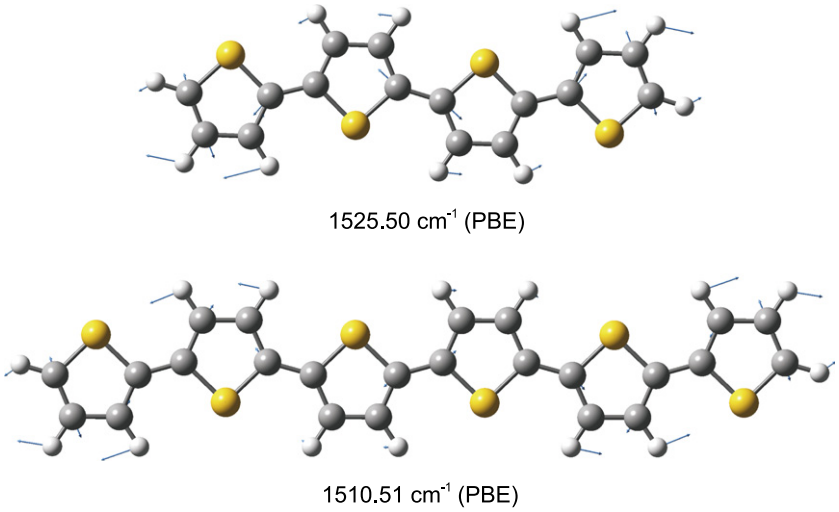

Fig. 12. In-plane Raman modes of the teramer and hexamer corresponding to the experimental peaks located at 1515 and 1504 cm^{-1} [10], calculated with the PBE functional.

A representative feature for all studied oligomer sizes is measured around 1050 cm^{-1} and it is both IR and Raman-active. It involves in-plane C—H motions and, even though it is not very intense, it is well reproduced by our calculations, which predict its position at 1052.9 cm^{-1} in the Raman spectrum of the hexamer [10,22].

For the tetramer, the double IR peaks around 1200 cm^{-1} are again better reproduced both as positions and intensities by the PBE functional. The B3LYP functional yields instead just one peak with a discrete shoulder (Fig. 4). The experimental IR mode measured at 1196 cm^{-1} for hexathiophene is predicted by the PBE calculations at 1211.80 cm^{-1} and is dominated, as mentioned above, by in-plane angle bendings involving the H atoms connected to the terminal cycles (Fig. 9).

The 1400–1600 cm^{-1} region is characterized mainly by in-plane combinations of longitudinal motions of the H atoms with in-ring stretching vibrations of the C=C double bonds. Significant IR modes of the dimer, tetramer, and hexamer are located in experiments at 1498, 1494, and 1493 cm^{-1}, respectively [10,22], and are closely reproduced by our PBE calculations. As one can observe in Fig. 10, which depicts the corresponding displacements of the tetramer and hexamer, the calculated frequency is blue shifted roughly by just 1%. The corresponding trimer mode manifests itself both in the IR and Raman spectra.

Two other experimental in-plane Raman-active modes occur at 1460 cm^{-1} for the tetramer and at 1458 cm^{-1} for the hexamer [10]. Our PBE calculations reproduce the experimental frequencies with

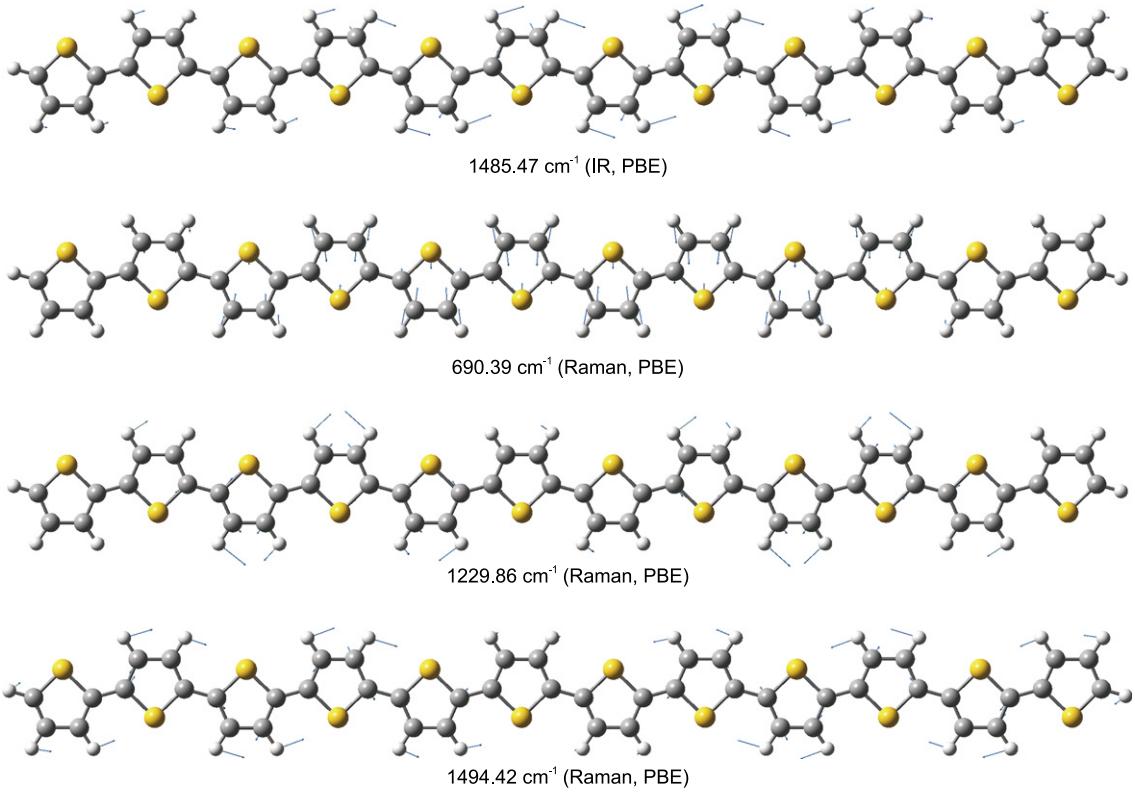

Fig. 13. In-plane and out-of-plane IR and Raman modes of the dodecamer obtained with the PBE functional.

even better accuracy than in the dimer case, namely the relative errors drop to approximately 0.5% for the tetramer and to 0.1% for the hexamer (see Fig. 11). In the case of the hexamer, the peak calculated at 1455.57 cm^{-1} matches fairly the experimental Raman data provided by other groups: Bazzaoui et al. at 1455 cm^{-1} [26], Loi et al. at 1459 cm^{-1} [27], Weinberg-Wolf et al. at 1461 cm^{-1} [28], and Brillante et al. at 1460 cm^{-1} [29].

For the frequency range beyond 1600 cm^{-1}, the Raman spectra appear similar for all three even-sized oligomers and are dominated by two strong in-plane modes. The dimer exhibits two peaks, the highest in intensity is experimentally measured at 1441 cm^{-1} and the other at 1553 cm^{-1}. The best agreement with the experiments is provided again by the PBE functional. For the tetramer and hexamer, the higher intensity peak is found at slightly higher frequencies (by less than 0.7%) than the experimental ones (see Fig. 11). For the tetramer, besides the terminal cycles, also the central pair of rings appears to be active (upper panel of Fig. 12). However, the corresponding hexamer vibration elucidates that, in fact, the *two terminal cycles* on each side of the chain are predominantly active and, with increasing oligomer size this behavior is accompanied also by a slight red shift of the frequencies.

A technical aspect which needs to be stressed again, this time in connection with the IR and Raman vibrations of the oligomers up to the dodecamer, is that above 1000 cm^{-1} the PBE functional performs consistently more realistically than B3LYP, continuing the trends which have been already established up to hexamer. The particular displacement patterns of the modes located around 1490 cm^{-1} in the IR and Raman spectra can be seen in Fig. 13. An interesting feature of the dodecamer concerns the fact that both the IR and Raman modes activate significantly the thiophene cycles situated in the proximity of the inversion point. On the contrary, for the smaller oligomers the vibration energy is distributed evenly over the chains or concentrated around the ends. Overall, from the PBE-based calculations the IR spectra result slightly red shifted and the Raman spectra marginally blue shifted (see Figs. 4 and 5).

4. Conclusions

We report on DFT computational investigations of the IR and Raman-active vibrations of polythiophenes with up to 12 cycles and match the results against experimental evidence from the literature.

We have assessed the performance of various combinations of exchange–correlation functionals and basis sets and all final interpretations have resulted from calculations based on the B3LYP and PBE functionals in conjunction with the 6-31G(d) basis set with imposed symmetry.

As a general remark concerning the equilibrium structures of the oligothiophenes, the C—C distances between in-ring atoms are consistently better reproduced by the PBE functional but, on the other hand, the inter-ring C—C and in-ring C—S bond lengths are better reproduced by the B3LYP functional. The bandgaps calculated for the 12 considered thiophenes show a monotonic decreasing trend with increasing chain size and for the B3LYP functional they converge towards the hexathiophene bandgap resulting from the measurements.

Regarding the IR and Raman vibrations, it is worth noting that we achieved with both functionals an agreement with the experiments which is superior to previous reports, even without applying any frequency scaling. However, the two employed functionals appear to be working optimally in complementary domains. Concretely, the B3LYP functional produces better agreement with the experiments mainly in the lower frequency range (below 1000 cm^{-1}), in particular in describing the out-of-plane modes which are predominant in this domain. On the other hand, the PBE functional performs significantly better in the intermediate and higher frequency domain (above 1000 cm^{-1}), where the frequencies predicted for the prevailing in-plane vibrations match remarkably the experimental values. This is particularly apparent for the Raman spectra, where the C=C in-plane vibrations are significant and the deviations from the experimental frequencies remain typically below 1%.

The IR and Raman spectral features corresponding to in-plane and out-of-plane vibrations develop gradually with increasing polymer size and show no significant difference between successive even and odd oligothiophenes. Corroborated with experimental condensed phase spectra, the IR and Raman frequencies calculated for different chain lengths provide an qualitative image on the relative positioning, i.e. stacking or lying, of the polythiophene chains with respect to the substrate.

Acknowledgments

The present work was funded by the POSDRU/88/1.5/S/60185 program and by the CNCSIS-UEFISCSU Project Number PNII-ID PCCE_129/2008.

References

[1] N.C. Greenham, A.R. Brown, D.D.C. Bradley, R.H. Friend, Electroluminescence in poly(3-alkylthienylene)s, Synth. Met. 57 (1993) 4134–4138.
[2] G. Horowitz, P. Delannoy, H. Bouchriha, F. Deloffre, J.L. Fave, F. Garnier, R. Hajilaoui, M. Heyman, F. Kouki, P. Valat, V. Wintgens, A. Yassar, Two-layer light-emitting diodes based on sexithiophene and derivatives, Adv. Mater. 6 (1994) 752–755.
[3] K. Okada, Y.-F. Wang, T. Nakaya, Yellow organic electroluminescent device based on novel thiophene Al complex as an emitting layer, Thin Solid Films 342 (1999) 8–10.
[4] A. Dodabalapur, Z. Bao, A. Makhija, J.G. Laquidanum, V.R. Raju, Y. Feng, H.E. Katz, J. Rogers, Organic smart pixels, Appl. Phys. Lett. 73 (1998) 142–144.
[5] J. Sakai, T. Taima, K. Saito, Efficient oligothiophene:fullerene bulk heterojunction organic photovoltaic cells, Org. Electron. 9 (2008) 582–590.
[6] R. Tipnis, J. Bernkopf, S. Jia, J. Krieg, S. Li, M. Storch, D. Laird, Large-area organic photovoltaic module—fabrication and performance, Solar Energy Mater. Solar Cells 93 (2009) 442–446.
[7] Conjugated polymeric materials: opportunities in electronics, in: J.L. Bredas, R.R. Chances (Eds.), Optoelectronics and Molecular Electronics, Kluwer Academic, Dordrecht, 1990.
[8] Y. Ohmori, H. Takahashi, T. Kawai, K. Yoshino, Gas-sensitive junction characteristics of poly(3-alkylthiophene) Schottky diodes, Jpn. J. Appl. Phys. 29 (1990) L1849–L1852.
[9] W.E. Torruellas, D. Neher, R. Zanoni, G.I. Stegeman, F. Kajzar, M. Leclerc, Dispersion measurements of the third-order nonlinear susceptibility of polythiophene thin films, Chem. Phys. Lett. 175 (1990) 11–16.
[10] A. Degli Esposti, O. Moze, C. Taliani, J.T. Tomkinson, R. Zamboni, F. Zerbetto, The intramolecular vibrations of prototypical polythiophenes, J. Chem. Phys. 104 (1996) 9704–9718.
[11] A. Degli Esposti, M. Fanti, M. Muccini, C. Taliani, G. Ruani, The polarized infrared and Raman spectra of a-T6 single crystal: an experimental and theoretical study, J. Chem. Phys. 112 (2000) 5957–5969.
[12] M.J. Frisch, G.W. Trucks, H.B. Schlegel, G.E. Scuseria, M.A. Robb, J.R. Cheeseman, J.A. Montgomery, Jr., T. Vreven, K.N. Kudin, J.C. Burant, J.M. Millam, S.S. Iyengar, J. Tomasi, V. Barone, B. Mennucci, M. Cossi, G. Scalmani, N. Rega, G.A. Petersson, H. Nakatsuji, M. Hada, M. Ehara, K. Toyota, R. Fukuda, J. Hasegawa, M. Ishida, T. Nakajima, Y. Honda, O. Kitao, H. Nakai, M. Klene, X. Li, J.E. Knox, H.P. Hratchian, J.B. Cross, C. Adamo, J. Jaramillo, R. Gomperts, R.E. Stratmann, O. Yazyev, A.J. Austin, R. Cammi, C. Pomelli, J.W. Ochterski, P.Y. Ayala, K. Morokuma, G.A. Voth, P. Salvador, J.J. Dannenberg, V.G. Zakrzewski, S. Dapprich, A.D. Daniels, M.C. Strain, O. Farkas, D.K. Malick, A.D. Rabuck, K. Raghavachari, J.B. Foresman, J.V. Ortiz, Q. Cui, A.G. Baboul, S. Clifford, J. Cioslowski, B.B. Stefanov, G. Liu, A. Liashenko, P. Piskorz, I. Komaromi, R.L. Martin, D.J. Fox, T. Keith, M.A. Al-Laham, C.Y. Peng, A. Nanayakkara, M. Challacombe, P.M.W. Gill, B. Johnson, W. Chen, M.W. Wong, C. Gonzalez, J.A. Pople, Gaussian 03, Revision B. 01, Gaussian Inc., Pittsburgh, PA, 2003
[13] A.D. Becke, J. Chem. Phys. 98 (1993) 5648;
C. Lee, W. Yang, R.G. Parr, Phys. Rev. B 37 (1988) 785–789.
[14] J.P. Perdew, K. Burke, M. Ernzerhof, Phys. Rev. Lett. 77 (1996) 3865–3868.
[15] L. Cuff, M. Kertesz, Evidence of quinonoid structures in the vibrational spectra of thiophene based conducting polymers: poly(thiophene), poly(thieno[3,4-b]benzene), and poly(thieno[3,4-b]pyrazine), J. Chem. Phys. 106 (1997) 5541–5553.
[16] G. Horowitz, B. Bachet, A. Yassar, P. Lang, F. Demanze, J.-L. Fave, F. Garnier, Growth and characterization of sexithiophene single crystals, Chem. Mater. 7 (1995) 1337–1341.

[17] S.M. Bouzzinea, M. Hamidi, M. Bouachrine, Density functional theory study of electroactive materials based on thiophene in their neutral and doped states, J. Appl. Chem. Res. 11 (2009) 40–46.
[18] K.-F. Braun, S.W. Hla, Charge transfer in the TCNQ-sexithiophene complex, J. Chem. Phys. 129 (2008). 064707-1-7.
[19] S.E. Koh, B. Delley, J.E. Medvedeva, A. Facchetti, A.J. Freeman, T.J. Marks, M.A. Ratner, Quantum chemical analysis of electronic structure and n- and p-type charge transport in perfluoroarene-modified oligothiophene semiconductors, J. Phys. Chem. B 110 (2006) 24361–24370.
[20] S. Pesant, P. Boulanger, M. Cote, M. Ernzerhof, Ab initio study of ladder-type polymers: polythiophene and polypyrrole, Chem. Phys. Lett. 450 (2008) 329–334.
[21] T.C. Chung, J.H. Kaufman, A.J. Heeger, F. Wudl, Charge storage in doped poly(thiophene): optical and electrochemical studies, Phys. Rev. B 30 (1984) 702–710.
[22] H. Goktas, F.G. Ince, A. Iscan, I. Yildiz, M. Kurt, I. Kaya, The molecular structure of plasma polymerized thiophene and pyrrole thin films produced by double discharge technique, Synth. Met. 159 (2009) 2001–2008.
[23] K. Shizu, T. Sato, K. Tanaka, Vibronic coupling density analysis for a-oligothiophene cations: a new insight for polaronic defects, Chem. Phys. 369 (2010) 108–121.
[24] M.H. Palmer, Comparison of theoretical and experimental studies of infrared spectral data for the 5-membered ring heterocycles, J. Mol. Struct. 834 (2007) 113–128.
[25] P. Hermet, N. Izard, A. Rahmani, Ph. Ghosez, Raman scattering in crystalline oligothiophenes: a comparison between density functional theory and bond polarizability model, J. Phys. Chem. B 110 (2006) 24869–24875.
[26] E.A. Bazzaoui, G. Levi, S. Aeiyach, J. Aubard, J.P. Marsault, P.G. Lacaze, SERS spectra of polythiophene in doped and undoped states, J. Phys. Chem. 99 (1995) 6628–6634.
[27] M.A. Loi, Q. Cai, H.R. Chandrasekhar, M. Chandrasekhar, W. Graupner, G. Bongiovanni, A. Mura, C. Botta, F. Garnier, High pressure study of the intramolecular vibrational modes in sexithiophene single crystals, Synth. Met. 116 (2001) 321–326.
[28] J.R. Weinberg-Wolf, L.E. McNeil, Resonant Raman spectroscopy on a-hexathiophene single crystals, Phys. Rev. B 69 (2004). 125202-1-4.
[29] A. Brillante, I. Bilotti, C. Albonetti, J.-F. Moulin, P. Stoliar, F. Biscarini, D.M. de Leeuw, Confocal Raman spectroscopy of a-sexithiophene: from bulk crystals to field-effect transistors, Adv. Funct. Mater. 17 (2007) 3119–3127.